Journal of Engineering Physics and Thermophysics, Vol. 68, No. 4, 1995

HYDRODYNAMIC CONTACT BETWEEN A ROTATING ROLL AND A SEMIPERMEABLE TRAY

V. M. Shapovalov

UDC 532.516

A viscous fluid flow in the gap between a side surface of a rotating roll and a rectangular cavity with a semipermeable bottom surface is considered in the Reynolds approximation.

The considered problem deals with the flow of a processed material in a rotor-type granulator consisting of two unidirectionally rotating cylinders. The inner solid cylinder is positioned eccentrically with respect to the outer perforated one (an inner contact of cylinders) [1]. Moreover, the present study may be useful when analyzing the flow in the gap of a two-screw extruder (an outer contact of impermeable cylinders) [2]. Hydrodynamic contact of an infinite cylinder with a semipermeable surface is considered in [3].

The flow scheme is given in Fig. 1. The tray filled with viscous fluid (a rectangular open channel) with a semipermeable bottom surface of width S moves translationally at a velocity W. A roll with a radius R is immersed into the channel. U is the peripheral velocity of the cylindrical surface. The side gaps between the roll ends and the channel walls are equal. The minimum gap h_0 in the z direction is constant. The x axis lies on a semipermeable surface. The y axis passes through the roll axis. The fluid flow in the end gaps is neglected. Trajectories of fluid particles lie in the planes perpendicular to the zaxis; therefore, there is no flow in the z direction ($v_z = 0$). With zero end gaps ($\delta = 0$) and different velocities ($U \neq W$) on the lines $z = 0$, $y = h$ and $z = S$, $y = h$ the gradient of shear velocity is infinite and, on determining the consumed power, we have a diverging Fourier series [4]. Therefore, in the end gaps of finite value, $\delta > 0$, a linear distribution of an axial velocity is assumed. At $U = W$ it may be supposed that $\delta = 0$. At the flow zone outlet x_1 the cavitation condition $\partial P/\partial x = 0$ is taken for pressure [5]. At points x_0, x_1 and under the semipermeable surface there is atmospheric pressure which is assumed to be equal to zero. For the conditions S, $h \ll x_1 - x_0$ shear stresses dominate in the gap and the pressure is uniform in the channel cross section ($\partial P/\partial y = \partial P/\partial x = 0$) but it changes in the longitudinal direction $P(x)$. The permeability of the bottom wall is described by the empirical dependence $v_y = -KP$ at $y = 0$. The medium is incompressible. The flow is steady-state. Mass and inertia forces are neglected.

In view of the assumptions adopted the problem is described by the system of equations

$$\frac{1}{\mu}\frac{dP}{dx} = \frac{\partial^2 v_x}{\partial y^2} + \frac{\partial^2 v_x}{\partial z^2}, \tag{1}$$

$$\frac{\partial v_x}{\partial x} + \frac{\partial v_y}{\partial y} + \frac{\partial v_z}{\partial z} = 0, \tag{2}$$

$$y = 0, \quad v_x = W, \quad v_y = -KP, \tag{3}$$

$$y = h, \quad v_y = U\frac{x}{R}, \quad v_x = \begin{cases} W + \dfrac{(U-W)}{\delta} z, & 0 \le z \le \delta, \\ U, & \delta \le z \le S - \delta, \\ W + \dfrac{(U-W)}{\delta}(S - z), & S - \delta \le z \le S, \end{cases} \tag{4}$$

Volgograd Technical University. Translated from Inzhenerno-Fizicheskii Zhurnal, Vol. 68, No. 4, pp. 612-618, July-August, 1995. Original article submitted December 13, 1993.

 1062-0125/95/6804-0500$12.50

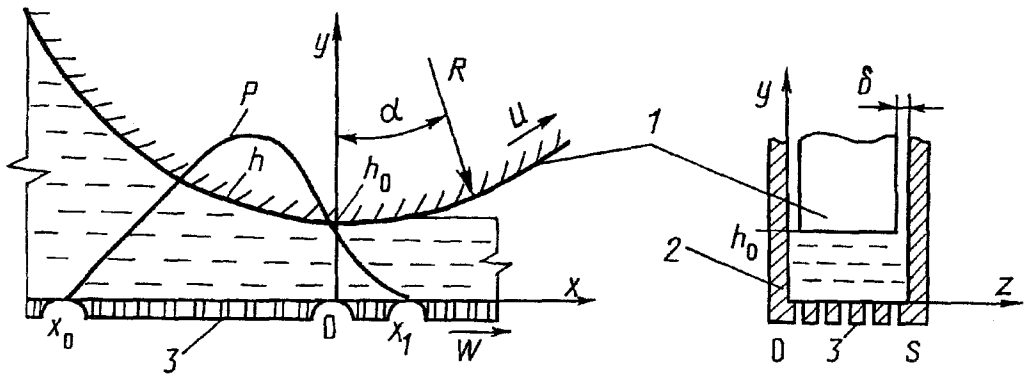

Fig. 1. Flow scheme: 1, roll; 2, rectangular tray; 3, semipermeable wall.

$$z = 0, \quad z = S, \quad v_y = 0, \quad v_x = W, \tag{5}$$

$$x = x_0, \quad P = 0, \quad x = x_1, \quad P = dP/dx = 0. \tag{6}$$

Conditions (4) are obtained for the case $\sin\alpha = x/R \ll 1$, since $U_y = U\sin\alpha = Ux/R$; $v_x = U\cos\alpha \approx U$. We integrate (2) in the region bounded by the sections x and x_1, surfaces $y = 0$ and $y = h(x)$, and walls $z = 0$ and $z = S$. Using conditions (3) and (4) for v_y, we can write

$$\int_0^S \int_x^{x_1} \int_0^h \frac{\partial v_x}{\partial x} dydxdz + \int_0^S \int_x^{x_1} (U\sin\alpha + KP)\, dxdz + \int_0^S \int_x^{x_1} \int_0^h \frac{\partial v_z}{\partial z} dydxdz = 0.$$

Then, allowing for the relationships

$$\frac{\partial}{\partial x}\int_0^h v_x dy = \int_0^h \frac{\partial v_x}{\partial x} dy + \frac{dh}{dx} v_x(h), \quad \frac{dh}{dx} v_x(h) = \tan\alpha\, U\cos\alpha,$$

$$\frac{\partial}{\partial z}\int_0^h v_z dy = \int_0^h \frac{\partial v_z}{\partial z} dy + \frac{dh}{dz} v_z(h), \quad \frac{dh}{dz} = 0, \quad v_z = 0,$$

we obtain an intergral form of the discontinuity equation

$$\int_0^S \int_0^h v_x dydz = \int_0^S \int_0^{h(x_1)} v_x(x_1)\, dydz + SK \int_x^{x_1} Pdx. \tag{7}$$

The axial fluid flow in the cross section is composed of the axial flow at the channel outlet and of the flow seeping through the semipermeable bottom surface.

In an arbitrary cross section Eqs. (1), (3)-(5) describe the Dirichlet problem for the Poisson equation. The solution of this problem by the Fourier method [6] gives the axial velocity profile in an arbitrary cross section

$$v_x = W + \frac{4S^2}{\pi^3\mu}\frac{dP}{dx}\sum_{n=1,3,\ldots}^{\infty} \frac{\sin\frac{\pi nz}{S}}{n^3}\left[\frac{\operatorname{ch}\frac{\pi n}{2S}(2y-h)}{\operatorname{ch}\frac{\pi nh}{2S}} - 1\right] +$$

$$+ \frac{4S(U-W)}{\pi^2\delta}\sum_{n=1,3,\ldots}^{\infty} \frac{\sin\frac{\pi nz}{S}}{n^2}\frac{\operatorname{sh}\frac{\pi ny}{S}}{\operatorname{sh}\frac{\pi nh}{S}}\left[\sin\frac{\pi n\delta}{S} - 2\pi n\sin^2\left(\frac{\pi n\delta}{2S}\right)\right]. \tag{8}$$

At $x = x_0$, $z = S/2$, $v_x < 0$, fluid circulation occurs at the flow zone outlet.

We introduce the dimensionless variables and the parameters

$$\rho = \frac{x}{\sqrt{2Rh_0}}, \quad \lambda = \frac{x_1}{\sqrt{2Rh_0}}, \quad \rho_0 = \frac{x_0}{\sqrt{2Rh_0}}, \quad \overline{P} = \frac{Ph_0^2}{W\mu\sqrt{2Rh_0}},$$

$$\Gamma = \frac{2K\mu R}{h_0^2}, \quad f = \frac{U}{W}, \quad \Delta = \frac{\delta}{S}, \quad q = \frac{h_0}{S}.$$

Substituting (8) into (7), we obtain the equation for pressure

$$\lambda^2 - \rho^2 + D\frac{d\overline{P}}{d\rho} + (f-1)B + \Gamma\int_{\rho}^{\lambda}\overline{P}d\rho = 0, \tag{9}$$

where

$$D = \frac{1}{12q^2}\left\{1 + \rho^2 - \frac{192}{\pi^3 q}\sum_{n=1,3,\ldots}^{\infty}\frac{\text{th}\left[\frac{\pi n}{2}q(1+\rho^2)\right]}{n^5}\right\};$$

$$B = \frac{8}{\Delta\pi^4 q}\sum_{n=1,3,\ldots}^{\infty} n^{-4}\left[\sin\pi n\Delta - 2\pi n\sin^2\left(\frac{\pi n\Delta}{2}\right)\right]\times$$

$$\times\left\{\text{th}\left[\frac{\pi nq}{2}(1+\lambda^2)\right] - \text{th}\left[\frac{\pi nq}{2}(1+\rho^2)\right]\right\}.$$

In Eq. (9) the parabolic approximation for the gap height was used: $h = h_0(1+\rho^2)$ [7].

The velocity of the efflux through the perforated bottom surface is uniform over the channel width, since $\partial P/\partial z = 0$. The fluid flow through this surface is determined by the integral

$$Q = SK\int_{x_0}^{x_1} Pdx = h_0 SWTI_1, \tag{10}$$

where

$$I_1 = \int_{\rho_0}^{\lambda}\overline{P}d\rho.$$

The bouyancy force affecting the roll from the fluid side is

$$F = S\int_{x_0}^{x_1} Pdx = \frac{2SW\mu R}{h_0}I_1. \tag{11}$$

From (10), (11) we have for permeability $K = Q/F$.

The consumed power can be determined by shear stresses affecting the channel walls from the fluid side [8]:

$$N = \mu\int_{x_0}^{x_1}\left[\int_0^S v_x\frac{\partial v_x}{\partial y}\Big|_0^h dz + 2W\int_0^h\frac{\partial v_x(z=S)}{\partial z}dy\right]dx,$$

or, with account for (8)

$$\frac{Nh_0}{2W^2\mu S\sqrt{2Rh_0}} = I_2 + \int_{\rho_0}^{\lambda}\left\{\frac{4(f-1)}{\pi^3 q}\frac{d\overline{P}}{d\rho}\sum_{n=1,3,\ldots}^{\infty} n^{-3}\,\text{th}\left[\frac{\pi nq(1+\rho^2)}{2}\right] +\right.$$

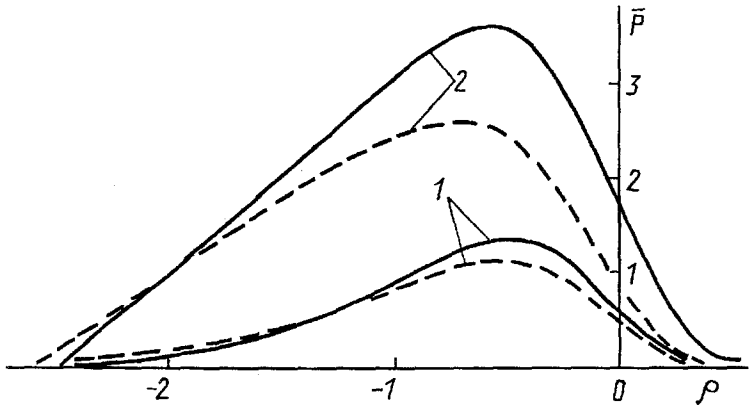

Fig. 2. Pressure diagrams in the channel: solid lines, $\Gamma = 0$; dashed lines, 0.2; 1, $q = 0$; 2, 0.4.

$$+\frac{4(f-1)^2 q}{\pi^2 \Delta}\sum_{n=1,3,\ldots}^{\infty}\frac{\operatorname{cth}[\pi n q(1+\rho^2)]}{n^2}\left[\sin\pi n\Delta - 2\pi n\sin^2\left(\frac{\pi n\Delta}{2}\right)\right]\Bigg\}d\rho\,, \tag{12}$$

where

$$I_2 = -\int_{\rho_0}^{\lambda}\bar{P}\rho d\rho\,.$$

Friction in the gaps between the channel side walls and the roll ends is disregarded.

We analyze in detail the case of equality of surface velocities $U = W$ at zero side gaps $\Delta = 0$. Considering the integrals I_1, I_2 in (9)-(12) as functions of the lower limit of integration, we obtain for pressure and the mentioned integrals a system of differential equations of first order

$$\frac{d\bar{P}}{d\rho} = \frac{\rho^2 - \lambda^2 - \Gamma I_1}{D}\,,\quad \frac{dI_1}{d\rho} = -\bar{P}\,,\quad \frac{dI_2}{d\rho} = \bar{P}\rho\,,$$

$$\rho = \lambda\,,\quad \bar{P} = I_1 = I_2 = 0\,,\quad \rho = \rho_0\,,\quad \bar{P} = 0\,.$$

The analysis is performed by the Runge-Kutta method. The calculations were started at an *a priori* assigned point $\rho = \lambda$ and ended at the point $\rho < \rho_0$, where the function $\bar{P}$ attained a negative value. A step over ρ is 0.05. The values of ρ_0, I_1, I_2 were determined by interpolation of $\bar{P}$ in the vicinity of the inversion point. The value $q = 0$ corresponds to an infinite roll width ($S = \infty$) and the relation

$$\lim_{q\to 0} D = \frac{(1+\rho^2)^3}{12}\,.$$

holds.

Figure 2 presents the calculated pressure profiles at different values of q and flow zone length $\lambda - \rho_0 \cong 3$. In the case of an infinitely wide roll ($q = 0$) the pressure gradient and the pressure itself at the beginning of the flow zone are insignificant. As q increases (converging of the side walls) the pressure gradient at the beginning of the flow zone grows and the maximum pressure increases: thus, at $q = 1$, $\Gamma = 0$ it reaches $\bar{P} = 11$ (not shown in the figure). With increase in the permeability of the bottom surface, the pressure decreases. Fluid friction on the side walls enhances the pressure effect typical of the roll processes, which is manifested itself in an increase of the pressure gradient in a minimum gap and in the flow section behind a minimum gap. Friction on the side walls increases fluid flow through the semipermeable surface since it is proportional to the area of the pressure diagram. Fluid flow through the bottom surface also increases with the length of the flow zone. Thus, at $\Gamma = 0.1$, $q = 0.2$ growth of $\lambda - \rho_0$ from 3.06 to 7.17 increases I_1 from 2.76 to 11.32. Correspondingly, the consumed power characterized by I_2 grows from 3.38 to 24.5.

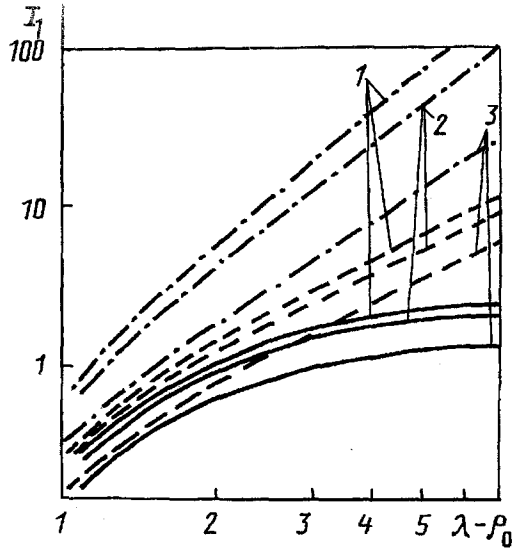

Fig. 3. Dependence of I_1 on the flow zone length: solid lines, $q = 0$; dashed lines, 0.2; dot-and-dash lines, 1; 1, $\Gamma = 0$; 2, 0.1; 3, 1.

In Fig. 3 the effect of the parameters q, Γ, $\lambda-\rho_0$ on the parameter I_1 characterizing the flow through the semipermeable surface (10) and the thrust force (11) are shown. Fluid friction on the side walls qualitatively changes the dependence. For an infinitely wide roll ($S = \infty$, $q = 0$) the existence of a limiting buoyancy force, power consumed, and flow seeping through a semipermeable surface is typical. This was noted in [9]. Thus, at $q = 0$ and with an increase of $\lambda - \rho_0$ from 5 to 7 the parameter I_1 changes slightly. This flow property is also confirmed by Fig 2, where the curves at $q = 0$ at the beginning of the flow zone are rather flat. An intense flow is localized in the vicinity of a minimum gap and, as the flow zone length increases, the area of the pressure diagram changes slightly. When $q > 0$, a monotonously growing dependence on $\lambda - \rho_0$ is characteristic for I_1; therefore virtually any quantity of fluid fed to the channel inlet will be pressed through a semipermeable surface. Consequently, the buoyancy force affecting the roll surface is proportional to the quantity of fluid supplied to the inlet.

The efficiency of granulator operation can be determined by the output-to-consumed power ratio, or, in dimensionless form, I_1/I_2. With $\lambda - \rho_0$ changing from 1 to 7, this index decreases from 3 to ~ 0.9 (for $q = 0$) and to ~ 0.4 (for $q \leq 1$, $0 < \Gamma \leq 1$). Friction on the side walls reduces the efficiency of granulator operation.

In fluid flow in a rotor-type granulator the forces of viscous friction are considerably greater than the inertia forces, the empty weight, and the centrifugal forces; therefore, the latter are not taken into account. Thus, from the data of [1] the following estimates are admissible: $R_2 = 0.32$ m; $\omega_1 \sim \omega_2 \sim 0.5$ rad/sec; $\rho_c \sim 10^3$ kg/m ; $\mu \sim 5 \cdot 10^3$ Pa·sec; $R_2\omega_2^2 \ll g$; $\mathrm{Re} \sim R_2\omega_2 R_2\rho_c/\mu \ll 1$. When using the given flow model for calculating granulators with an inner contact of two cylinders [1] $W = \omega_2 R_2$ should be considered as the peripheral velocity of the perforated cylinder, and $U = \omega_1 R_1$ as the circumferential velocity of the rotor. The calculated radius providing the transition to the scheme of Fig. 1 is $R = R_2R_1/(R_2 - R_1)$, and a minimum gap is $h_0 = R_2 - R_1$.

Thus, the hydrodynamic effect of the channel side walls is manifested in the suppression of the fluid counterflow at the inlet, increase of the initial pressure gradient, and growth of the thrust force and fluid flow rate through the semipermeable wall.

NOTATION

x, y, z, Cartesian coordinates; U, peripheral velocity of the roll; W, translational velocity of the tray; h, gap height; h_0, minimum gap; δ, side gap, v_x, v_y, v_z, velocity components; K, coefficient of channel wall permeability; P, $\overline{P}$, dimensional and dimensionless pressures; R, roll radius; S, channel width; μ, fluid viscosity; α, angle; x_0, x_1, ρ_0, λ, dimensional and dimensionless coordinates of the flow zone boundaries; Γ, dimensionless permeability; f, friction; Δ, q, geometrical simplexes; ρ, dimensionless variable; Q, bulk flow rate of fluid; F,

buoyancy force; N, power; I_1, I_2, integral parameters of flow; ω_1, ω_2, angular velocities of rotor and cylinder; ρ_c, fluid density, q, gravity acceleration; Re, Reynolds number; R_1, R_2, radii of cylinder and rotor in a granulator.

REFERENCES

1. T. A. Partalin and O. N. Ivanov, Development, study, and calculation of machines and apparatuses of the chemical industry. Mezhvuz. Sb., Moscow (1980), pp. 121-125.
2. N. I. Basov and V. Broi (Editors), Technology of Processing Plastics [in Russian], Moscow (1985).
3. V. M. Shapovalov et al., Inzh.-Fiz. Zh., **54**, No. 3, 415-422 (1988).
4. V. I. Yankov, V. P. Pervadchuk, and V. I. Boyarchenko, Processing Fibre-Forming Polymers [in Russian], Moscow (1989).
5. M. A. Galakhov, P. B. Gusyatnikov, and A. P. Novikov, Mathematical Models of Contact Hydrodynamics [in Russian], Moscow (1985).
6. L. V. Kantorovich and V. I. Krylov, Approximate Methods of Higher Analysis [in Russian], Moscow-Leningrad (1962).
7. D. M. McKelvi, Processing of Polymers [Russian translation], Moscow (1965).
8. B. D. Vechter, B. M. Shapovalov, and N. V. Tyabin, Plastmassy, No. 9, 39-40 (1991).
9. V. V. Khokhlov and V. M. Shapovalov, Mathematical simulation in the processes of production and processing of polymers. Extended Abstracts of the 2nd Regional Scientific-Engineering Conference, Perm (1992), p. 2.